Cofactor Dependence of Reduction Potentials for [4Fe-4S]$^{2+/1+}$ in Lysine 2,3-Aminomutase†

Glen T. Hinckley and Perry A. Frey*

Department of Biochemistry, College of Agricultural and Life Sciences, University of Wisconsin, 1710 University Avenue, Madison, Wisconsin 53726

Received September 27, 2005; Revised Manuscript Received January 11, 2006

ABSTRACT: Lysine 2,3-aminomutase (LAM) catalyzes the interconversion of L-lysine and L-β-lysine by a free radical mechanism. The 5′-deoxyadenosyl radical derived from the reductive cleavage of *S*-adenosyl-L-methionine (SAM) initiates substrate-radical formation. The [4Fe-4S]$^{1+}$ cluster in LAM is the one-electron source in the reductive cleavage of SAM, which is directly ligated to the unique iron site in the cluster. We here report the midpoint reduction potentials of the [4Fe-4S]$^{2+/1+}$ couple in the presence of SAM, *S*-adenosyl-L-homocysteine (SAH), or 5′-{*N*-[(3*S*)-3-aminocarboxypropyl]-*N*-methylamino}-5′-deoxyadenosine (*aza*SAM) as measured by spectroelectrochemistry. The reduction potentials are −430 ± 2 mV in the presence of SAM, −460 ± 3 mV in the presence of SAH, and −497 ± 10 mV in the presence of *aza*SAM. In the absence of SAM or an analogue and the presence of dithiothreitol, dihydrolipoate, or cysteine as ligands to the unique iron, the midpoint potentials are −479 ± 5, −516 ± 5, and −484 ± 3 mV, respectively. LAM is a member of the radical SAM superfamily of enzymes, in which the CxxxCxxC motif donates three thiolate ligands to iron in the [4Fe-4S] cluster and SAM donates the α-amino and α-carboxylate groups of the methionyl moiety as ligands to the fourth iron. The results show the reduction potentials in the midrange for ferredoxin-like [4Fe-4S] clusters. They show that SAM elevates the reduction potential by 86 mV relative to that of dihydrolipoate as the cluster ligand. This difference accounts for the SAM-dependent reduction of the [4Fe-4S]$^{2+}$ cluster by dithionite reported earlier. Analogues of SAM have a weakened capacity to raise the potential. We conclude that the midpoint reduction potential of the cluster ligated to SAM is 1.2 V less negative than the half-wave potential for the one-electron reductive cleavage of simple alkylsulfonium ions in aqueous solution. The energetic barrier in the reductive cleavage of SAM may be overcome through the use of binding energy.

Lysine 2,3-aminomutase (LAM)[1] from *Clostridium subterminale* SB4 catalyzes the interconversion of L-α-lysine and L-β-lysine according to Scheme 1 (*1*). The rearrangement pattern entails a 2,3-nitrogen shift and a concomitant 3,2-hydrogen shift initiated by the 5′-deoxyadenosyl radical, analogous to adenosylcobalamin-dependent rearrangements (*2*). However, the source of the 5′-deoxyadenosyl radical in the action of LAM is not adenosylcobalamin; rather, it arises through the reversible one-electron reductive cleavage of *S*-adenosyl-L-methionine (SAM, Scheme 2A). A [4Fe-4S] center in the 1+ oxidation state supplies the electron for the reductive homolytic cleavage of the bond linking the sulfur and C-5′ of the ribose moiety in SAM to give the 5′-deoxyadenosyl radical and methionine (*3*). Reductive cleavage of SAM is increasingly recognized in the actions of other enzymes, including biotin synthase (*4*), lipoyl synthase (*5*), anaerobic ribonucleotide reductase activating enzyme (*6*), and pyruvate formate lyase activating enzyme (*7*), all of which cleave SAM to produce the 5′-deoxyadenosyl radical, which then abstracts a hydrogen atom from a substrate. An analysis of the NTSB database has indicated that a number of other uncharacterized enzymes may also employ this unique chemistry (*8*).

Scheme 1

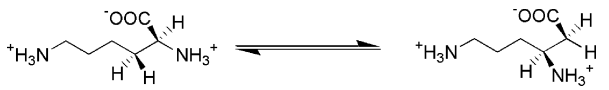

The [4Fe-4S] cluster in LAM is coordinated by three cysteine residues in a conserved CX_3CX_2C motif. Although a fourth coordinating protein-based ligand is not ruled out, it is believed that the fourth iron is available for coordination of a substrate or conenzyme (*9*), as in aconitase and related hydrolyase enzymes (*10*, *11*). Evidence of unique iron ligands includes the following: (a) Mild oxidation of the [4Fe-4S] cluster with ferricyanide results in a [3Fe-4S] cluster (*12*), indicative of a non-cysteinyl-coordinated iron (*13*). (b) XAS data indicate that the selenium of selenomethionine in *Se*-adenosyl-L-selenomethionine becomes directly coordinated

† This research was supported by Grant DK28607 from the National Institute of Diabetes and Digestive and Kidney Diseases and by NIH Grant 5 T32 GM08349.

* To whom correspondence should be addressed. Telephone: (608) 262-0055. E-mail: frey@biochem.wisc.edu.

[1] Abbreviations: LAM, lysine 2,3-aminomutase; SAM, *S*-adenosyl-L-methionine; XAS, X-ray absorption spectroscopy; ENDOR, electron nuclear double resonance; SAH, *S*-adenosyl-L-homocysteine; *aza*SAM, 5′-{*N*-[(3*S*)-3-aminocarboxypropyl]-*N*-methylamino}-5′-deoxyadenosine; EPPS, *N*-(2-hydroxyethyl)piperazine-*N*′-3-propanesulfonic acid; PLP, pyridoxal 5′-phosphate; DTT, dithiothreitol; DHL, dihydrolipoate; HPLC, high-performance liquid chromatography; EPR, electron paramagnetic resonance; BCA, bicinchoninic acid; NHE, normal hydrogen electrode.

10.1021/bi0519497 CCC: $33.50
Published on Web 02/17/2006

Scheme 2

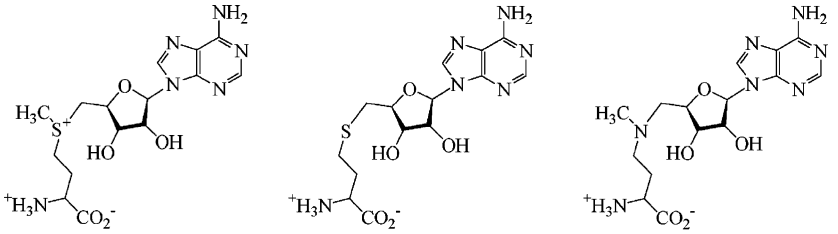

A. *S*-adenosyl-L-methionine (SAM) **B.** *S*-adenosyl-L-homocysteine (SAH) **C.** *aza*SAM

to an iron site in the cluster after homolytic cleavage of the carbon−selenium bond (*14*). (c) Data from ENDOR spectroscopy reveal that the carboxyl and amino groups of the methionine moiety of SAM are ligated directly to a unique iron site in the $[4Fe\text{-}4S]^{2+}$ cluster (*15*). The binding of SAM in this fashion presumably facilitates inner sphere electron transfer between the iron−sulfur cluster and the sulfonium center in SAM.

An interesting feature of the [4Fe-4S] cluster in LAM is that the spectroscopic observation of the 1+ oxidation state upon reduction of the 2+ state is facilitated by the presence of SAM or a structural analogue such as *S*-adenosyl-L-homocysteine (SAH, Scheme 2B) (*3*). A reasonable hypothesis accounting for this effect is that the binding of SAM or SAH to the enzyme raises the midpoint reduction potential[2] of the $[4Fe\text{-}4S]^{2+}$ center (*16*). However, the means by which this may occur is not known. It may be that coordination of the carboxyl and amino groups of SAM to an iron site in the center raises the reduction potential of the $[4Fe\text{-}4S]^{2+/1+}$ couple.

The reduction of SAM and the concomitant homolytic cleavage of the carbon−sulfur bond constitute a high-energy reaction. Colichman and Love performed the definitive work on the one-electron reduction of sulfonium ions in aqueous solution and determined the half-wave potential of a trialkyl sulfonium ion to be −1.6 V (*17*). If the half-wave potential for the reductive cleavage of SAM at the enzymatic site were similar to this value, then the participating $[4Fe\text{-}4S]^{1+}$ cluster would have to display a comparable reduction potential for significant equilibrium amounts of the 5′-deoxyadenosyl radical to be produced. This problem might be overcome if the cleavage of SAM were coupled to a thermodynamically downhill process quenching the radical. However, the dominant steady-state species resulting from SAM cleavage is the β-lysyl-related radical, not a stable structure (*2*, *16*). In any case, knowledge of the redox behavior of the iron−sulfur cluster will be necessary to define the chemistry of this process. Therefore, we sought to measure the midpoint reduction potentials of the $[4Fe\text{-}4S]^{2+/1+}$ couple in the presence of SAM or structural analogues. We further determined the midpoint potentials in the absence of SAM and the presence of sulfhydryl compounds, and we present the results in this paper.

EXPERIMENTAL PROCEDURES

Materials. 5′-{*N*-[(3*S*)-3-Aminocarboxypropyl]-*N*-methylamino}-5′-deoxyadenosine (*aza*SAM, Scheme 2C), synthesized as described in ref *18*, was a generous gift from G. M. Blackburn. Mediators 4,4′-dimethyl-1,1′-trimethylene-2,2′-dipyridyl bromide and 1,1′-trimethylene-2,2′-dipyridyl bromide were synthesized according to the method of Salmon and Hawkridge (*19*). All other chemicals were purchased from Sigma or Aldrich at the highest available purity and used as supplied.

Enzyme Expression and Purification. Recombinant clostridial LAM was expressed in *Escherichia coli* as described previously (*20*). Purification was based on previous procedures (*21*, *22*) with minor modifications. The cells were lysed and centrifuged as described previously (*21*). Polyethyleneimine replaced streptomycin sulfate as the DNA-precipitating agent. After Q-Sepharose chromatography, the enzyme was precipitated with 70% $(NH_4)_2SO_4$ and resuspended in 30 mM EPPS (pH 8.0) containing 0.1 mM lysine, 10 μM PLP, and 1 mM DTT. The protein was desalted by gel filtration chromatography over a 29 cm × 2.5 cm column of Sephadex S-300 equilibrated with the buffer described above.

Iron−Sulfur Reconstitution. Reconstitution of the [4Fe-4S] cluster in LAM was performed according to the procedure of Hewitson et al. (*23*) with some modifications. Desalted recombinant LAM was concentrated with Centriprep YM-30 spin (Millipore) concentrators to a concentration of no more than 10 mg/mL. To this was added a 6-fold molar excess over active sites of Na_2S and $Fe(NH_4)SO_4$ in 30 mM EPPS (pH 8.0) with 5 mM DTT. The reconstitution mixture was held at room temperature for 6−12 h inside a Coy anaerobic chamber. Then the mixture was gel filtered over a 29 cm × 2.5 cm column of Sephadex S-300 equilibrated with buffer containing 30 mM EPPS (pH 8.0), 0.1 mM lysine, 10 μM PLP, and 1 mM DTT to quantitatively separate the precipitated iron sulfide from the reconstituted LAM, which emerged in a dark brown band. This eluate was again concentrated on Centriprep YM-30 concentrators. The iron content was measured by the method of Kennedy et al. (*24*). The sulfide content was measured by the method of Beinert (*25*).

In two experiments, the iron−sulfur clusters were not reconstituted, but LAM containing its normal complement of [4Fe-4S] clusters was reductively incubated by the published procedure for activating the enzyme, either as described with DHL (*3*) or by substituting 50 mM cysteine for DHL. Cysteine was at least as effective in reductive activation as DHL. The resulting enzymes were coulometrically titrated to measure the midpoint reduction potentials using the procedures described below.

Activity Assays. LAM was assayed for activity as described in Miller et al. (*26*). Aliquots were taken at 2 min intervals and the reactions quenched with 2 M perchloric acid. These were then derivatized with phenyl isothiocyanate and chro-

[2] All potentials are quoted versus the normal hydrogen electrode.

matographed by reverse-phase HPLC using a 4 mm × 250 mm C-8 column from Vydac to separate the phenyl isothiocyanated derivatives of L-lysine and L-β-lysine.

Reductive Titration Procedure. Spectroelectrochemical titrations were run as previously described (*27*). Each titration mixture contained 2 mg (3.5 nmol) of reconstituted LAM (or reductively incubated LAM), 150 mM EPPS (pH 8.0), 200 mM KCl (as an electrolyte), 100 μM 4,4′-dimethyl-1,1′-trimethylene-2,2′-dipyridyl bromide, 100 μM 1,1′-trimethylene-2,2′-dipyridyl bromide, and the appropriate adenosyl cofactor at 42 μM. Each sample was reduced at an applied voltage in the range of −800 to −650 mV (vs Ag/AgCl) for 15 min. The potential was monitored to ensure stability, and the sample was then transferred into an EPR tube and frozen in cold isopentane (ca. −56 °C). EPR samples were stored in liquid nitrogen until they were analyzed. The Ag/AgCl electrode was standardized against a saturated calomel electrode ($E°$ = 241.5 mV) before and after each series of reductions. Post-EPR analysis, protein concentrations were quantitated by the BCA assay (Pierce Endogen) calibrated to a standard curve generated from the original titration mixture.

EPR Spectroscopy. Equipment used for EPR spectroscopy is the same as that described previously (*3*). EPR conditions for each sample are described in the figure legends.

Data Analysis. Because of the lack of an EPR signal from the $[4Fe\text{-}4S]^{2+}$ form of the enzyme, the data were fitted to a nonlinear form of the Nernst equation, including only the intensity of the reduced form.

$$I_{red} = I_{max} \times e^{(E_m - E)/v}/[1 + e^{(E_m - E)/v}] \quad (1)$$

where I_{red} is the signal intensity, I_{max} is the maximal signal intensity (for a completely reduced sample), E_m is the midpoint potential of the cluster, E is the measured potential of the system, and $v = RT/nF$, which is 25.8 mV for a one-electron process at 26 °C. While v can be fitted with this equation, we have simplified the fitting by setting the value to 25.8 mV.

RESULTS

Reconstitution of LAM. Previous preparations of LAM contained iron and sulfur corresponding to approximately 2 equiv of iron and sulfide per subunit (*3*). EPR analysis indicated that nearly all of the paramagnetic iron was in the form of [4Fe-4S] clusters (*12*). However, more recent preparations of hexahistidine-tagged recombinant LAM contained ~3 equiv of iron and sulfide per subunit; this was attributed to improved growth and purification techniques (*28*). These observations, coupled with the knowledge that each subunit contains the appropriate three-cysteine motif for binding a [4Fe-4S] cluster (*20*), led us to believe that each subunit of LAM contains one [4Fe-4S] cluster in vivo, with some of them having been lost during purification. Therefore, we reconstituted the clusters by a published method.

The iron and sulfide content of the reconstituted enzyme turned out to be 3.8 ± 0.4 Fe/subunit and 4.3 ± 0.3 S^{2-}/subunit, respectively. In addition, reconstitution removed an extraneous species tentatively assigned as $[4Fe\text{-}4S]^{3+}$ on the basis of its EPR signal. The optimal time required for removal of all $[4Fe\text{-}4S]^{3+}$ signal was a minimum of 6 h. The specific activity of the resulting LAM was 69−70 IU/mg, significantly higher than those previously reported (*3*, *20*).

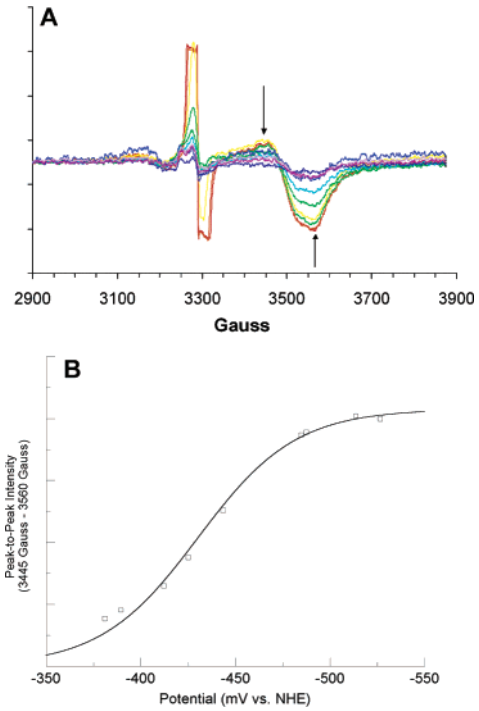

FIGURE 1: Titration of the $[4Fe\text{-}4S]^{1+}$ cluster in the presence of SAM. (A) 10 K EPR spectra from coulometric titration. Arrows denote the two magnetic field values used for peak-to-peak intensity determinations. Spectra were computed averages of four 2 min scans with a time constant of 0.3 s. Spectra were recorded at 9.256 GHz, with a modulation amplitude of 16 G, a power of 1 mW, and a gain of 8000. (B) Potential vs peak-to-peak intensity. The best fit curve of the data to eq 1 is shown. Signal intensities were normalized for protein concentrations by means of a BCA protein assay (see the text). The large, off-scale g = 2.0 signal is radical content due to the mediator.

Coulometric Titration in the Presence of SAM, SAH, and AzaSAM. [4Fe-4S] clusters physiologically tend to traverse one oxidative couple (either 3+/2+ or 2+/1+), and the second couple is generally not observed under physiological conditions (*29*−*32*). In LAM, the 2+/1+ transition is associated with activation of the enzyme (*3*).

The reconstituted LAM, with iron−sulfur clusters in the form of $[4Fe\text{-}4S]^{2+}$, was titrated coulometrically in the presence of SAM, SAH, or *aza*SAM. In the titration with SAM, the potential range was from −381 to −526 mV (vs NHE). The resulting EPR spectra recorded at 10 K are overlaid in Figure 1A. Peak-to-peak differences computed between prominent features at 3455 G (g = 1.91) and 3560 G (g = 1.86) are plotted against the measured potentials and fitted to eq 1 in Figure 1B. The EPR spectra for the coulometric titration of LAM in the presence SAH, within the potential range of −428 to −528 mV, are shown in Figure 2A. The peak-to-peak intensity differences computed between 3415 G (g = 1.94) and 3470 G (g = 1.91) are plotted and fitted in Figure 2B as described above. The EPR spectra for the coulometric titration of LAM in the presence of *aza*SAM within the potential range of −433 to −520 mV are shown in Figure 3A. The peak-to-peak intensity differences computed between 3410 G (g = 1.94) and 3575 G (g

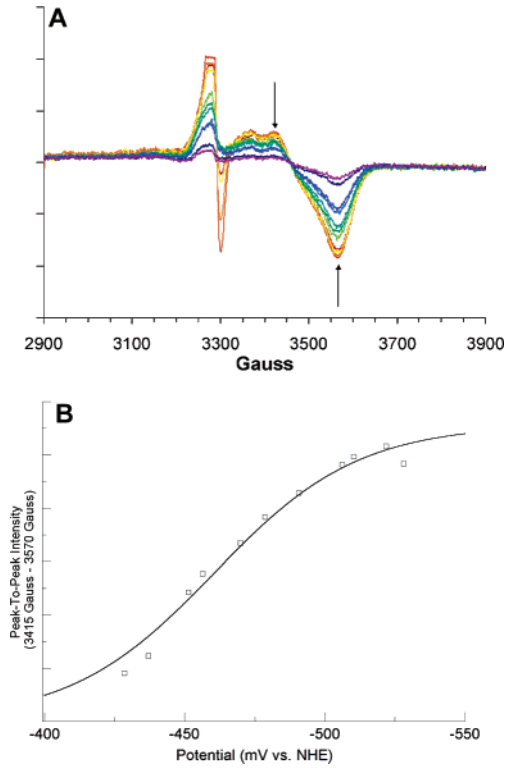

FIGURE 2: Titration of the $[4Fe\text{-}4S]^{1+}$ cluster in the presence of SAH. (A) 10 K EPR spectra from coulometric titration. Arrows denote the two magnetic field values used for peak-to-peak intensity determinations. Spectra were computed averages of four 2 min scans with a time constant of 0.3 s. Spectra were recorded at 9.256 GHz, with a modulation amplitude of 16 G, a power of 1 mW, and a gain of 8000. (B) Potential vs peak-to-peak intensity. The best fit curve of the data to eq 1 is shown. Signal intensities were normalized for protein concentrations by means of a BCA protein assay (see the text).

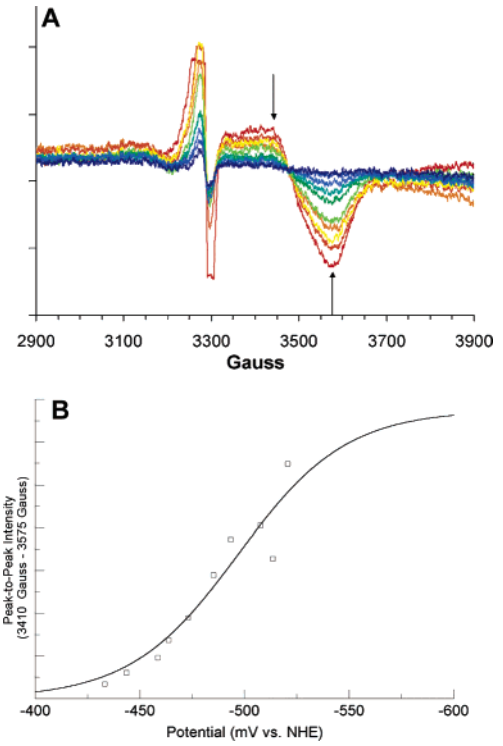

FIGURE 3: Titration of the $[4Fe\text{-}4S]^{1+}$ cluster in the presence of *aza*SAM. (A) 10 K EPR spectra from coulometric titration. Arrows denote the two magnetic field values used for peak-to-peak intensity determinations. Spectra were computed averages of four 2 min scans with a time constant of 0.3 s. Spectra were recorded at 9.256 GHz, with a modulation amplitude of 16 G, a power of 1 mW, and a gain of 8000. (B) Potential vs peak-to-peak intensity. The best fit curve of the data to eq 1 is shown. Signal intensities were normalized for protein concentrations by means of a BCA protein assay (see the text).

= 1.85) are plotted and fitted as described above in Figure 3B. The midpoint potentials for the couples are included in Table 1.

Figure 4A shows the coulometric titration results, within the potential range of −475 to −600 mV, for LAM that had not been reconstituted with iron and sulfide but had been activated by reductive incubation with DHL, as described previously (*3*). In panel B, the peak-to-peak intensity differences between 3415 G (g = 1.94) and 3515 G (g = 1.88) are replotted and fitted to eq 1. The resulting midpoint potential is entered in the second line of Table 1.

The midpoint potentials in the first three lines of Table 1 are for LAM in the absence of SAM or an analogue. The first line is for reconstituted LAM, which contains DTT (*27*), and the second and third lines are for un-reconstituted LAM that has been activated by reductive incubation with either DHL or cysteine, respectively.

Cofactor Ligation of the Unique Iron: Effects on the EPR Spectra. The α-amino and carboxylate groups of SAM ligate the unique iron in the [4Fe-4S] cluster of activated LAM (*15*). The same ligands are available in SAH and *aza*SAM. The low-temperature EPR spectra of LAM reduced in the presence of SAM, SAH, and *aza*SAM (shown in Figure 5A−C, respectively) are similar but significantly different, because of structural differences among SAM and the analogues. Thus, the EPR spectral envelope is very sensitive to the nature of the ligands to the unique iron in the [4Fe-4S] cluster.

Table 1: Midpoint Reduction Potentials of the $[4Fe\text{-}4S]^{2+/1+}$ Couple in Lysine 2,3-Aminomutase

form	midpoint reduction potential (mV vs NHE)
as-reconstituted	-479 ± 5[a]
DHL reduction[b]	-516 ± 5
cysteine reduction[c]	-484 ± 3
reconstituted plus SAM	-430 ± 2
reconstituted plus SAH	-460 ± 3
reconstituted plus *aza*SAM	-497 ± 10

[a] Previously reported in ref *27*. [b] Reductively incubated with DHL (*3*). [c] Reductively incubated as described in ref *3* but with 50 mM cysteine in place of DHL.

Spectrum D is the low-temperature EPR spectrum of the $[4Fe\text{-}4S]^{1+}$ cluster in LAM in which the cluster has been reconstituted in the presence of $Fe(NH_3)SO_4$, Na_2S, and DTT. Spectra E and F are the low-temperature EPR spectra of the $[4Fe\text{-}4S]^{1+}$ cluster in LAM activated by reductive incubation with DHL and cysteine, respectively. The spectra are significantly different from one another and from those obtained in the presence of SAM or its analogues. In the simplest and most obvious interpretation of the spectral variations, the differences may be attributed to the different ligands contributed by DTT in the reconstituted enzyme and by DHL or cysteine in the reductively activated samples.

DISCUSSION

Measurement of the midpoint reduction potential of the $[4Fe\text{-}4S]^{2+/1+}$ couple in LAM is a necessary first step toward

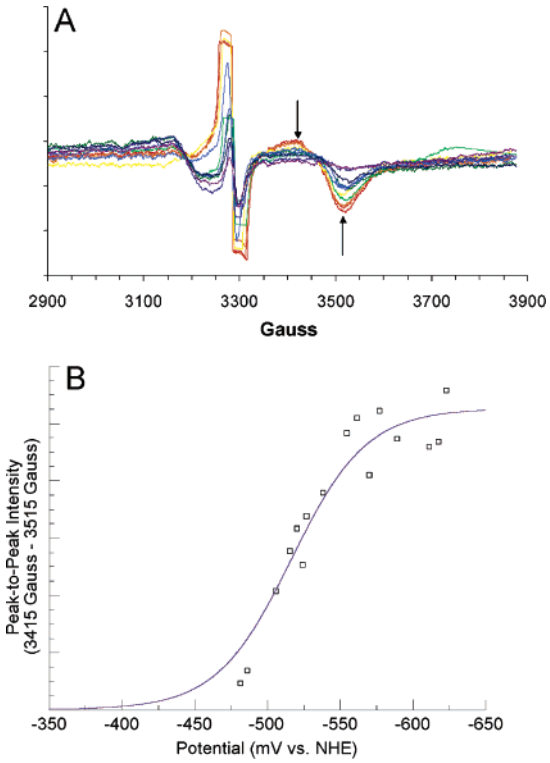

FIGURE 4: Titration of the $[4Fe\text{-}4S]^{1+}$ cluster in the presence of DHL. (A) 10 K EPR spectra from coulometric titration. Arrows denote the two magnetic field values used for peak-to-peak intensity determinations. Spectra were computed from spectra collected as described in preceding figure legends. (B) Potential vs peak-to-peak intensity. The best fit curve of the data to eq 1 is shown. Signal intensities were normalized for protein concentrations by means of a BCA protein assay (see the text).

elucidating the mechanism of the reductive cleavage of SAM. First, the apparent SAM dependence in the $[4Fe\text{-}4S]^{2+/1+}$ transition seen previously indicates a SAM-dependent shift in the reduction potential (*3*, *16*). Second, the energetic requirements for the one-electron reductive cleavage of the sulfonium group in SAM raise fundamental questions about how a biological iron−sulfide center could function in this capacity: The reduction potential of the [4Fe-4S] center might be lowered, that of SAM might be elevated, or both might be perturbed. These results verify that SAM and also SAH elevate the midpoint potential for the $[4Fe\text{-}4S]^{2+/1+}$ couple in the active site of LAM, explaining the early observation of SAM dependence in this transition. Thus, SAM facilitates the reduction of the iron−sulfur cluster.

The 50−86 mV positive elevation in midpoint potential brought about by the presence of SAM might be attributed to an electrostatic effect of the sulfonium group. Anions tend to stabilize the ferric form of iron more than the ferrous form, resulting in a more negative reduction potential (*33*). Conversely, the presence of a cation in the proximity of the iron center should elevate the reduction potential, as the ferrous form would be thermodynamically less destabilized than the ferric form. While SAM elevates the midpoint potential for the iron−sulfur center in the case of LAM, this effect cannot be attributed solely to the sulfonium group because SAH also brings about a significant elevation while lacking the positively charged sulfonium center. The reduction potential of the $[4Fe\text{-}4S]^{2+/1+}$ couple brought about by the presence of SAM is 30 mV more positive than that in the presence of SAH, and 50 mV more positive than that for the enzyme reconstituted in the presence of DTT. Therefore, the positive charge may exert a modest effect; however, both SAM and SAH elevate the reduction potential, as shown by these results, and both facilitate reduction (*3*).

Scheme 3

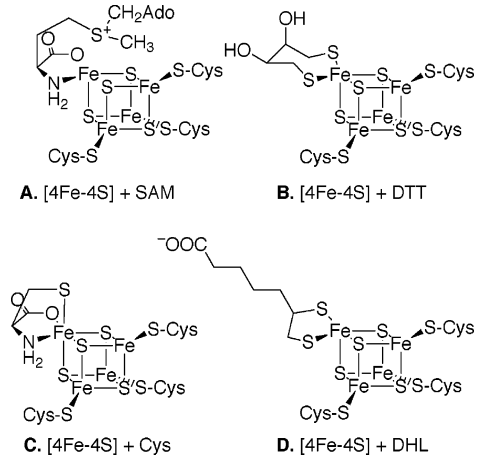

The 20 mV lowering of the midpoint potential in the presence of *aza*SAM highlights the complexities of the effects of SAM analogues on the reduction of the iron−sulfide center. The tertiary amine group in *aza*SAM would not be ionized under the conditions of these experiments (*28*), so *aza*SAM may be more analogous to SAH than to SAM from an electrostatic standpoint. However, in contrast to SAH, *aza*SAM depresses the reduction potential. The effects of SAM and its analogues on the reducing properties may be more related to alterations in the Fe−S bonding within the cluster than to electrostatics in the methionine side chain.

The midpoint potentials for LAM quoted in the first three lines of Table 1 were obtained in the absence of SAM or a SAM analogue. In the active enzyme, two ligands to the [4Fe-4S] cluster are contributed by the carboxylate and amino groups of the methionyl moiety of SAM (*15*), as illustrated in Scheme 3A. In the absence of SAM or a SAM analogue, the unique iron site in the [4Fe-4S] cluster must bind other ligands. In principle, these may be internal protein ligands or ligands from small molecules in the solution. If in the absence of SAM or an analogue the ligands are internal protein ligands, the low-temperature EPR spectra should be characteristic of the internal protein ligands and independent of the molecules in solution. However, in Figure 5, spectra D−F demonstrate that the spectra are sensitive to the nature of the thiol compounds in solution. The spectral differences are not consistent with internal protein ligands. Reconstituted LAM contains DTT, and the ligands are likely to be the thiol groups of DTT, as shown in Scheme 3B. In LAM reductively incubated with cysteine, the thiol, amino, and carboxylate groups of cysteine are likely to be the ligands (Scheme 3C). In the enzyme reductively incubated with DHL, the ligands are likely to be the thiol groups of DHL (Scheme 3D). DTT, DHL, and cysteine each contribute two negatively charged ligands, yet the midpoint potential with DHL is significantly more negative. Thus, as in the case of SAM and its analogues contributing ligands, electrostatics alone does not seem to determine the midpoint potentials in this series.

The earlier report of SAM dependence in the reduction of the $[4Fe\text{-}4S]^{2+}$ cluster can be explained by these results,

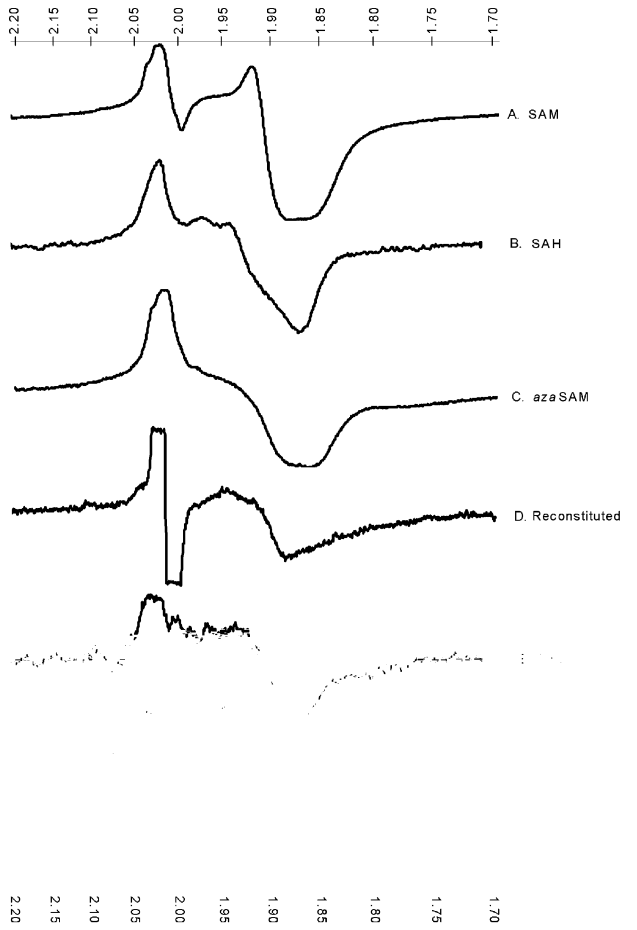

FIGURE 5: Low-temperature EPR spectra of the $[4Fe\text{-}4S]^{1+}$ cluster with various ligands to the unique iron. The ligands to the unique iron are as indicated in the figure. The scales at the top and bottom give *g* values. The spectrum for cysteine as the ligand is interrupted by a radical signal from the electron transfer mediator used in the electrolytic reduction. It is absent in the other spectra because dithionite was used as the reducing agent.

as set forth in Table 1. In the earlier work, LAM had been activated by reductive incubation with DHL, and 2 mM dithionite then produced a marginal low-temperature EPR signal for the $[4Fe\text{-}4S]^{1+}$ cluster (*3*). The additional presence of SAM elicited a strong signal. Table 1 shows that the midpoint potential in the presence of SAM is 86 mV less negative than in the presence of DHL alone. Thus, a SAM dependence for the reduction by dithionite is confirmed and quantitated. SAM displaces DHL from the unique iron site of the $[4Fe\text{-}4S]^{2+}$ cluster; consequently, the midpoint potential is elevated from −516 to −430 mV.

The iron−sulfur cluster in lysine 2,3-aminomutase performs a distinctive chemical feat, the one-electron reductive cleavage of a carbon−sulfur bond in a sulfonium ion (SAM) to initiate radical chemistry. This unique mode of radical initiation is an increasingly recognized phenomenon in the actions of a number of diverse enzymes (*9*). Reductive cleavage of SAM has stimulated efforts to devise a chemical model (*34*): synthetically constructed $[4Fe\text{-}4S]^{1+}$ clusters in organic solvents can reductively cleave sulfonium ions to give the respective thioether and alkanes as products. While there is much biochemical (*21*, *35*) and spectroscopic evidence (*36*) that the cluster can perform the one-electron reductive cleavage of the sulfonium of SAM, the extremely low potential (−1.6 V) needed for this reaction in solution stands in stark contrast to the observed range of midpoint reduction potentials for $[4Fe\text{-}4S]^{2+/1+}$ couples [from −300 to −700 mV (*37*)].

The midpoint potential for the cluster in LAM might have been at the low end of the range for [4Fe-4S] clusters, or alternatively, the midpoint reduction potential of the sulfonium center in SAM might be elevated to the range of the reduction potentials for ferredoxin-like clusters. These results show that the midpoint potential for the complex of LAM with SAM is in the midrange for $[4Fe\text{-}4S]^{2+/1+}$ transitions. Therefore, the reductive cleavage of SAM is not explained by a lowering of the reduction potential of the iron−sulfur cluster upon binding of SAM. Instead, SAM facilitates the reduction of the iron−sulfur cluster by elevating the midpoint potential. The difference of ∼1.2 V between the midpoint potential of the $[4Fe\text{-}4S]^{2+/1+}$ couple and the half-wave potential of the sulfonium center in SAM remains to be explained in molecular terms. Presumably, binding energy between the enzyme and other components of the reaction plays a role in facilitating electron transfer.

Biotin synthase is also a radical-SAM enzyme with a [4Fe-4S] cluster that reductively cleaves SAM, and it is the only other radical-SAM enzyme for which a midpoint potential for the reduction of the iron−sulfur center is available. The purified protein is deficient in iron and sulfide, and reconstitution generates two iron−sulfur clusters with reduction potentials of −440 and −505 mV (*38*). These values are in the range quoted here for LAM in the absence of SAM. Effects of SAM and SAM analogues have not been reported for biotin synthase.

ACKNOWLEDGMENT

We are grateful to Professor George H. Reed for making his EPR spectrometers available for this study.

REFERENCES

1. Chirpich, T. P., Zappia, V., Costilow, R. N., and Barker, H. A. (1970) Lysine 2,3-aminomutase, *J. Biol. Chem. 245*, 1778−1789.
2. Frey, P. A. (1990) Importance of Organic Radicals in Enzymatic Cleavage of Unactivated C−H Bonds, *Chem. Rev. 90*, 1343−1357.
3. Lieder, K. W., Booker, S., Ruzicka, F. J., Beinert, H., Reed, G. H., and Frey, P. A. (1998) *S*-Adenosylmethionine-Dependent Reduction of Lysine 2,3-aminomutase and Observation of the Catalytically Functional Iron−Sulfur Centers by Electron Paramagnetic Resonance, *Biochemistry 37*, 2578−2585.
4. Guianvarc'h, D., Florentin, D., Bui, B. T. S., Nunzi, F., and Marquet, A. (1997) Biotin Synthase, a New Member of the Familiy of Enzymes Which Uses *S*-Adenosylmethionine as a Source of Deoxyadenosyl Radical, *Biochem. Biophys. Res. Commun. 236*, 402−406.
5. Miller, J. R., Busby, R. W., Jordan, S. W., Cheek, J., Henshaw, T. F., and Ashley, G. W. (2000) *Escherichia coli* LipA is a Lipoyl Synthase: In Vitro Biosynthesis of Lipoylated Pyruvate Dehydrogenase Complex from Ocatnoyl-Acyl Carrier Protein, *Biochemistry 39*, 15166−15178.
6. Ollagnier, S., Mulliez, E., Schmidt, P. P., Eliasson, R., Gaillard, J., and Deronzier, C. (1997) Activation of the Anaerobic Ribonucleotide Reductase from *Escherichia coli*, *J. Biol. Chem. 272*, 24216−24223.
7. Henshaw, T. F., Cheek, J., and Broderick, J. B. (2000) The $[4Fe\text{-}4S]^{1+}$ Cluster of Pyruvate Formate-Lyase Activating Enzyme Generates the Glycyl Radical on Pyruvate Formate-Lyase: EPR-Detected Single, *J. Am. Chem. Soc. 122*, 8331−8332.
8. Sofia, H. J., Chen, G., Hetzler, B. G., Reyes-Spindola, J. F., and Miller, N. E. (2001) Radical SAM, a novel protein superfamily linking unresolved steps in familiar bisynthetic pathways with

radical mechanisms: Functional characterization, *Nucleic Acids Res. 29*, 1097−1106.
9. Cheek, J., and Broderick, J. B. (2001) Adenosylmethionine-dependent iron−sulfur enzymes: Versatile clusters in a radical new role, *J. Biol. Inorg. Chem. 6*, 209−226.
10. Kent, T. A., Dreyer, J. L., Kennedy, M. C., Huynh, B. H., Emptage, M. H., Beinert, H., and Munck, E. (1982) Mossbauer studies of beef heart aconitase: Evidence for facile interconversions of iron−sulfur clusters, *Proc. Natl. Acad. Sci. U.S.A. 79*, 1096−1100.
11. Flint, D. H., and Allen, R. M. (1996) Iron−Sulfur Proteins with Nonredox Functions, *Chem. Rev. 96*, 2315−2334.
12. Petrovich, R. M., Ruzicka, F. J., Reed, G. H., and Frey, P. A. (1992) Characterization of Iron Sulfur Clusters in Lysine 2,3-Aminomutase by Electron Paramagnetic Resonance Spectroscopy, *Biochemistry 31*, 10774−10781.
13. Holm, R. H., Kennepohl, P., and Solomon, E. I. (1996) Structural and Functional Aspects of Metal Sites in Biology, *Chem. Rev. 96*, 2239−2314.
14. Cosper, N. J., Booker, S., Ruzicka, F. J., Frey, P. A., and Scott, R. A. (2000) Direct FeS Cluster Involvement in Generation of a Radical in Lysine 2,3-Aminomutase, *Biochemistry 39*, 15668−15673.
15. Chen, D., Walsby, C., Hoffman, B. M., and Frey, P. A. (2003) Coordination and Mechanism of Reversible Cleavage of S-Adenosylmethionine by the [4Fe-4S] Center in Lysine 2,3-Aminomutase, *J. Am. Chem. Soc. 125*, 11788−11789.
16. Frey, P. A., and Booker, S. (1999) Radical Intermediates in the Reaction of Lysine 2,3-aminomutase, *Adv. Free Radical Chem. 2*, 1−43.
17. Colichman, E. L., and Love, D. L. (1953) Polarography of Sulfonium Salts, *J. Org. Chem. 18*, 40−46.
18. Thompson, M. J., Mekhalfia, A., Hornby, D. P., and Blackburn, G. M. (1999) Synthesis of Two Stable Nitrogen Analogues of *S*-Adenosyl-L-methionine, *J. Org. Chem. 64*, 7467−7473.
19. Salmon, R. T., and Hawkridge, F. M. (1980) The Electrochemical Properties of Three Dypyridinium Salts as Mediators, *J. Electroanal. Chem. 112*, 253−364.
20. Ruzicka, F. J., Lieder, K. W., and Frey, P. A. (2000) Lysine 2,3-Aminomutase from *Clostridium subterminale* SB4: Mass Spectral Chacterization of Cyanogen Bromide-Treated Peptides and Cloning, *J. Bacteriol. 182*, 469−476.
21. Moss, M. L., and Frey, P. A. (1990) Activation of Lysine 2,3-Aminomutase by *S*-Adenosylmethionine, *J. Biol. Chem. 265*, 18112−18115.
22. Petrovich, R. M., Ruzicka, F. J., Reed, G. H., and Frey, P. A. (1991) Metal Cofactors of Lysine 2,3-aminomutase, *J. Biol. Chem. 266*, 7656−7660.
23. Hewitson, K. S., Ollagnier-de Choudens, S., Sanakis, Y., Shaw, N. M., Baldwin, J. E., and Munck, E. (2002) The iron−sulfur center of biotin synthase: Site-drected mutants, *J. Biol. Inorg. Chem. 7*, 87−93.
24. Kennedy, M. C., Kent, T. A., Emptage, M., Merkle, H., Beinert, H., and Munck, E. (1984) Evidence for the formation of a linear [3Fe-4S] cluster in partially unfolded aconitase, *J. Biol. Chem. 259*, 14463−14471.
25. Beinert, H. (1983) Semi-micro Methods for Analysis of Labile Sulfide and of Labile Sulfide plus Sulfane Sulfur in Unusually Stable Iron−Sulfur Proteins, *Anal. Biochem. 131*, 373−378.
26. Miller, J., Bandarian, V., Reed, G. H., and Frey, P. A. (2001) Inhibition of Lysine 2,3-Aminomutase by the Alternative Substrate 4-Thialysine and Characterization of the 4-Thialysyl Radical Intermediate, *Arch. Biochem. Biophys. 387*, 281−288.
27. Hinckley, G., and Frey, P. A. (2006) Construction of a Spectroelectrochemical Titrator Adaptable to Multiple Spectroscopies, *Anal. Biochem. 349*, 103−111.
28. Hinckley, G. T., Ruzicka, F. J., Thompson, M. J., Blackburn, G. M., and Frey, P. A. (2003) Adenosyl coenzyme and pH dependence of the $[4Fe\text{-}4S]^{2+/1+}$ transition in lysine 2,3-aminomutase, *Arch. Biochem. Biophys. 414*, 34−39.
29. Carter, C. W., Jr., Kraut, J., Freer, S. T., Alden, R. A., Sieker, L. C., Adman, E. T., and Jensen, L. H. (1972) A comparison of Fe_4S_4 clusters in high-potential iron protein and in ferredoxin, *Proc. Natl. Acad. Sci. U.S.A. 69*, 3526−3529.
30. Cammack, R. (1973) "Super-Reduction" of Chromatium High-Potential Iron-Sulphur Protein in the Presence of Dimethyl Sulphoxide, *Biochem. Biophys. Res. Commun. 54*, 548−554.
31. Heering, H. A., Bulsink, Y. B. M., Hagen, W. R., and Meyer, T. E. (1995) Reversible super-reduction of the cubane [4Fe-4S]-(3+;2+;1+) in the high-potential iron−sulfur protein under non-denaturing conditions. EPR spectroscopic and electrochemical studies, *Eur. J. Biochem. 232*, 811−817.
32. Stephens, P. J., Morgan, T. V., Devlin, F., Penner-Hahn, J. E., Hodgson, K. O., Scott, R. A., Stout, C. D., and Burgess, B. K. (1985) [4Fe-4S]-cluster-depleted *Azotobacter vinelandii* ferredoxin I: A new 3Fe iron−sulfur protein, *Proc. Natl. Acad. Sci. U.S.A. 82*, 5661−5665.
33. Philips, C. S. G., and Williams, R. J. P. (1966) *Inorganic Chemistry*, Vol. II, Oxford University Press, New York.
34. Daley, C. J. A., and Holm, R. H. (2001) Reactivity of $[Fe_4S_4(SR)_4]^{2-/3-}$ Clusters with Sulfonium Cations: Analogue Reaction Systems for the Initial Step in Biotin Synthase Catalysis, *Inorg. Chem. 40*, 2785−2793.
35. Moss, M. L., and Frey, P. A. (1987) The Role of S-Adenosylmethionine in the Lysine 2,3-aminomutase Reaction, *J. Biol. Chem. 262*, 14859−14862.
36. Magnusson, O. T., Reed, G. H., and Frey, P. A. (2001) Characterization of an Allylic Analouge of the 5′-Deoxyadenosyl Radical: An Intermediate in the Reaction of Lyisne 2,3-Aminomutase, *Biochemistry 40*, 7773−7782.
37. Capozzi, F., Ciurli, S., and Luchinat, C. (1998) Coordination sphere versus protein environment as determinants of electronic and functional properties of iron−sulfur proteins, *Struct. Bonding 90*, 127−160.
38. Ugulava, N. B., Gibney, R. R., and Jarrett, J. T. (2001) Biotin Synthase Contains Two Distinct Iron−Sulfur Cluster Binding Sites: Chemical and Spectroelectrochemical Analysis of Iron−Sulfur Cluster Interconversions. *Biochemistry 40*, 8343−8351.

BI0519497